GEOMETRIC INVARIANTS FOR CLASSIFICATION OF CORTICAL SULCI

Monica K. Hurdal[*]*, Juan B. Gutierrez, Christian Laing*[†]*, Aaron D. Kline, Deborah A. Smith*

Florida State University, Department of Mathematics
Tallahassee, FL, USA 32306-4510
Email: mhurdal@math.fsu.edu

ABSTRACT

We have developed a computational method based on a family of geometric measures for the purpose of classification and identification of families of sulcal curves from human brain surfaces. Topologically correct cortical surfaces of the human brain were extracted from magnetic resonance images. Polygonal curves representing sulcal curves were then generated on each surface. Geometric measures including Gauss integrals, moments and topological features were computed for each curve to obtain a set of feature vectors in a high dimensional vector space. These feature were used to classify the curves into sulcal and hemispheric classes. In our preliminary results, an automatic differentiation between sulcal paths from the left or right hemispheres and individual sulcal curve classification were achieved, indicating these measures may have biological significance in neuroscientific data.

Index Terms— Geometric modeling, image shape analysis, magnetic resonance imaging, topology, biomedical computing

1. INTRODUCTION

Detecting similarities and differences in cortical features can lead to characterization of differences in populations, including detection of disease and aging-related changes. For instance, one-year changes in MRI brain volumes in older adults have been observed [1] as have gray matter losses in Alzheimer's disease [2]. Additionally, labeling cortical structures is critical for cartography and conveying information for comparing individual subjects or populations. Increasingly large sample sizes mandate the use of automated procedures that are sensitive to relevant anatomical features.

In this paper we present results of an automated method for computing geometric shape descriptors on polygonal curves representing sulci of the human brain. These descriptors or features provide a way to compare and measure similarity based on morphology. Using these descriptors, we were able to classify sulcal curves into left and right hemispheres, as well as distinguish the type of sulcal curve (e.g. central sulcus, superior frontal sulcus). These results indicate that the selected feature vectors represent promising characteristics for automatically parcellating sulcal curves.

[*]This work was supported in part by NIH Human Brain Project grant P20 EB02013. Thanks to D. Rottenberg, U. Minnesota for providing the MRI data and D.W. Sumners, Florida State U. for discussions about Gauss integral measures.

[†]Currently at New York University, Departments of Chemistry and Mathematics, NY, USA

2. METHODS

We are interested in shape descriptors which are *mathematical invariants*, meaning they are quantities which remain unchanged (i.e. invariant) under a given class of mathematical isometries. Invariants are extremely useful for classifying mathematical objects because they usually reflect intrinsic properties of the object of study. We generate piecewise linear discretized representations of continuous surfaces and curves and we present methods for computing these geometric shape descriptors in the discrete setting.

2.1. MRI Data and Sulcal Curves

High resolution 1.5 Tesla, T1-weighted MRI brain scans (0.86mm x 0.86mm x 1.00mm) from 15 subjects obtained from a static force experiment were used [3]. FreeSurfer [4], a freeware software package available to the neuroscience community, was used to perform a typical MRI processing pipeline including intensity corrections, skull and cerebellum stripping, hemisphere separation and topological cortical surface reconstruction of the gray matter/cerebrospinal fluid interface (referred to as the gray matter (GM) surface). Surfaces produced using FreeSurfer have been used to report results from a number of sensory and cognitive tasks, as well as for comparing diseased and control populations [5, 6].

Gyral ridges and sulcal fundus beds, which anatomically characterize the surface of the brain, can be efficiently captured using methods that involve curvature. A fundus bed (which we call a sulcal curve) is a path along a sulcus that has minimal negative curvature between two given points. Computational geometry methods are available for computing the principal curvatures of a discretized surface [7]. The sulcal paths presented in the paper were constructed using Dijkstra's algorithm [8, 9] using the following curvature cost function

for traveling from vertex v_i to v_j:

$$c_{ij}^{sulc} = \left(\frac{(\kappa_i + \kappa_{max})^2}{2} + \frac{(\kappa_j + \kappa_{max})^2}{2} + \frac{(\kappa_i - \kappa_j)^2}{6} \right) |e_{ij}|,$$

where $|e_{ij}|$ is the edge length between vertices v_i and v_j, κ_i and κ_j are the maximal of the principal curvatures for v_i and v_j, and κ_{max} is the maximal of the absolute value of the principal curvature for the surface.

Five sulci were traced on each cortical surface hemisphere for each subject: the central, precentral, calcarine, superior frontal and superior temporal sulci for a grand total of 150 sulci (15 subjects x 2 hemispheres x 5 sulci). A user identified a start and end point for each sulcus (which were verified by an independent user to reduce variability) and dynamic programming methods were used to automatically compute the path of principal curvature between these two points. All sulci were continuous with the exception of the precentral sulcus which is often separated into superior and inferior components [10].

2.2. Shape Descriptors

Since cortical sulci are a set of space curves, the methodology we propose is concerned with crossings seen in planar projections of curves. We propose the use of invariant geometric shape descriptors which consist of topological measures such as scaled Gauss integrals, thickness and ropelength, as well as moment-based measures.

2.2.1. Scaled Gauss integrals

Scaled Gauss integrals are measures of the self entanglement of curves in space and have proved to be useful in biopolymer classification [11]. One of the Gauss integral measures is the well known writhe number of a closed space curve γ [12] and another is the average crossing number. We computed a set of Gauss integral measures, up to third order, given by $I_{(1,2)}$, $I_{|1,2|}$, $I_{(1,2)(3,4)}$, $I_{|1,2|(3,4)}$, $I_{(1,2)|3,4|}$, $I_{|1,2||3,4|}$, $I_{(1,3)(2,4)}$, $I_{|1,3|(2,4)}$, $I_{(1,3)|2,4|}$, $I_{|1,3||2,4|}$, $I_{(1,4)(2,3)}$, $I_{|1,4|(2,3)}$, $I_{(1,4)|2,3|}$, $I_{|1,4||2,3|}$, $I_{(1,2)(3,4)(5,6)}$, $I_{(1,2)(3,5)(4,6)}$, $I_{(1,2)(3,6)(4,5)}$, $I_{(1,3)(2,4)(5,6)}$, $I_{(1,3)(2,5)(4,6)}$, $I_{(1,3)(2,6)(4,5)}$, $I_{(1,4)(2,3)(5,6)}$, as well as the arc length of the curve L, where

$$I_{|1,2|}(\gamma) = \sum_{0<i_1<i_2<|C|} |W(i_1, i_2)|,$$

$$I_{|1,3|(2,4)}(\gamma) = \sum_{0<i_1<\cdots<i_4<|C|} |W(i_1, i_3)| W(i_2, i_4),$$

etc., with $|C|$ equal to the total number of vertices in γ and

$$W(i_1, i_2) = \frac{1}{2\pi} \int_{i_1}^{i_1+1} \int_{i_2}^{i_2+1} w(t_1, t_2) dt_2 dt_1,$$

$$w(t_1, t_2) = \frac{[\gamma'(t_1), \gamma(t_1) - \gamma(t_2), \gamma'(t_2)]}{|\gamma(t_1) - \gamma(t_2)|^3},$$

for $t_1, t_2 \in [0, 1]$ and the numerator of $w(t_1, t_2)$ is the triple scalar product.

2.2.2. Thickness and ropelength

Intuitively, any non-intersecting smooth curve can be thickened into a smooth tube of constant radius and without self intersections [13, 14]. If the curve is a straight line then there is no upper bound, but for any other curve there is a maximal radius where the tube is not smooth or it has self intersections. This critical radius is the thickness of the curve, and is an intrinsic property of the curve. The thickness Δ of γ is defined by $\Delta(\gamma) = \min_{1 \le i \le |C|} \rho_G(v_i)$ where

$$\rho_G(v_i) = \min_{k \neq |C|; i \neq j \neq k \neq i} r(v_i, v_j, v_k)$$

and $r(v_i, v_j, v_k)$ is the unique circle radius given by three non-collinear vertices v_i, v_j, v_k. The ropelength of γ is given by $L/\Delta(\gamma)$ where L is the length of γ.

2.2.3. Moments

Moments can be used to discriminate space curves [15] and moment invariants have also been reported as a meaningful measure of brain structure [16]. Moments were calculated using the force moment M_{pqr} in $\mathbb{R}^3$ of order p in x, q in y and r in z which is given by

$$M_{pqr} = \sum_{i=1}^{|C|} x_i^p y_i^q z_i^r \sum_{j=1}^{\delta(v_i)} \frac{|e_{ij}|}{2} \mu,$$

where $\delta(v_i)$ is the degree of vertex v_i and μ is the mass per unit of length of each edge.

2.3. Data mining and classification

A set of features comprised of Gauss integrals, moment-based measures, thickness and ropelength were calculated for each sulcus. Each sulcus was then included into a possible class, such as a left hemisphere class or a calcarine sulcus class. Classification scenarios were tested to determine if the feature vectors were useful measures, resulting in a classification rate and a measure of classification error. We performed principal component analysis (PCA) and multiple discriminant analysis (MDA) [17] on the classification scenarios. In addition, we selected five widely used methods to define a discriminant function and classify the data using 90% of it with (10-fold) cross-validation [18, 19]. Cross-validation measures the performance of the prediction system in a self-consistent way by systematically leaving out a few sulci (about 10%) during the training process and testing the trained prediction system against those left-out sulci. This is repeated such that

Table 1. Classification between left and right hemispheres using moment-based measures. MAE stands for Mean Absolute Error. RAE stands for Relative Absolute Error.

Method	% Correct	MAE	RAE
Naive Bayes	98%	0.0235	5%
Naive Bayes Simple	98%	0.0236	5%
LMT	99%	0.1594	32%
Classific. Via Regression	99%	0.0421	8%
Simple Logistic	99%	0.1897	38%

every sulcus in the dataset is left out at least once. Compared to tests on independent sets, cross-validation has less bias and better predictive and generalization power. The calculation and application of all classifiers was done with Weka, an open source collection of machine learning algorithms for data mining [19].

3. RESULTS

We considered different feature vectors as the basis of sulcal classification, including Gauss integral measures, moment-based measures, and all features together. The sulcal curves were separated into two classes: sulcal curves on the left hemisphere and curves on the right hemisphere, giving 75 curves per class. Over 98% of the sulci were correctly classified. Table 1 gives a summary of the classification methods, percentage of correctly classified sulci and error measures. Attribute selection showed that over a set of 70 features, moment-based measures gave the overall best performance. Moment-based measures can be interpreted as providing information about the position of the curves in space. As a result, these measures are able to discriminate between curves located in the left and right hemispheres. Figure 1 shows PCA analysis of the data. There is a clear cluster separation for classes that belong to different hemispheres.

Scaled Gauss integrals proved to be an efficient set of measures to discriminate a sulcus within a single class (e.g. to discriminate between left calcarine sulci and right calcarine sulci). Figure 2 shows the MDA projection of the data. The performance with MDA indicates that it is possible to perform one-class hemispherical discrimination using only Gauss integrals.

4. DISCUSSION

It was possible to discriminate with great efficiency the hemisphere in which sulci were located. Moment-based measures give good performance due to their ability to discriminate position in space. Gauss integral measures were useful for differentiating the hemispheric location of a single sulcus. This promising result may indicate that Gauss integral invari-

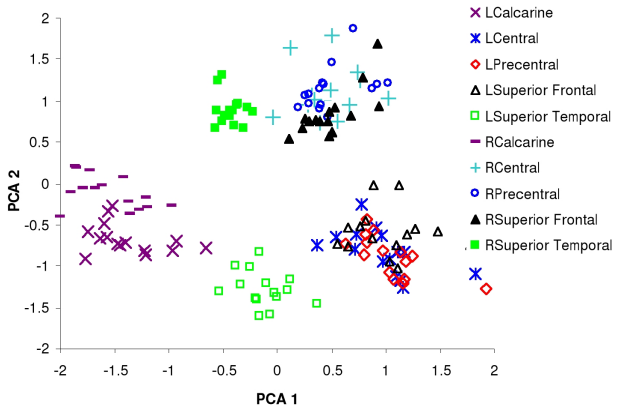

Fig. 1. Projection using PCA. Differentiation between sulci from the left and right hemispheres. Discrimination using moment-based measures.

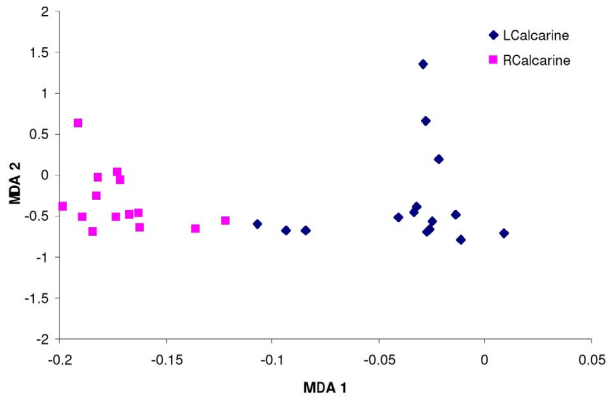

Fig. 2. Projection using MDA. Differentiation between sulci from the left and right hemispheres. Discrimination using Gauss integrals.

ants are potentially useful measures for characterizing cortical shape on a local, rather than global scale.

Since sulcal curves are close to planar, the Gauss integrals are close to zero. Large cortical variations in position are not captured by Gauss integrals since they are invariant under translation and rotation. However, they may capture more subtle local changes in shape such as those that occur within the same sulcus on different hemispheres. Gauss integrals have found biological significance in characterizing polygonal curves such as proteins. It is worthwhile to consider the possible application of these measures to neuroscientific data.

Gauss integrals are invariant under dilation, translation and rotation, but they are not invariant under reflection. Therefore, they could easily identify the hemisphere location of a sulcus. Moment invariants are useful for characterizing shape on a global scale. However, moment measures can be problematic since small variations in position, e.g. a subject taking an MRI with the head slightly tilted, can cause significant changes in the native moment magnitude. Thus, moments and Gauss integrals must be used in conjunction in order to obtain a reliable classification. The results presented here demonstrate that it is possible to obtain a good discrimination of sulcal paths using a family of geometric measures comprised of Gauss integrals and moment-based measures.

5. REFERENCES

[1] S. M. Resnick, A. F. Goldszal, C. Davatzikos, S. Golski, M. A. Kraut, E. J. Metter, R. N. Bryan, and A. B. Zonderman, "One-year age changes in *MRI* brain volumes in older adults," *Cerebral Cortex*, vol. 10, no. 5, pp. 464–472, 2000.

[2] P. M. Thompson, K. M. Hayashi, G. de Zubicaray, A. L. Janke, S. E. Rose, J. Semple, D. Herman, M. S. Hong, S. S. Dttmer, D. M. Doddrell, and A. W. Toga, "Dynamics of gray matter loss in alzheimer's disease," *Neuroscience*, vol. 23, no. 3, pp. 994–1005, 2003.

[3] S. LaConte, J. Anderson, S. Muley, J. Ashe, S. Frutiger, K. Rehm, L. K. Hansen, E. Yacoub, X. Hu, D. Rottenberg, and S. Strother, "The evaluation of preprocessing choices in single-subject BOLD fMRI using NPAIRS performance metrics," *NeuroImage*, vol. 18, pp. 10–27, 2003.

[4] A. M. Dale, B. Fischl, and M. I. Sereno, "Cortical surface-based analysis I: Segmentation and surface reconstruction," *NeuroImage*, vol. 9, pp. 179–194, 1999.

[5] L. F. Lyoo, Y. H. Sung, S. R. Dager, S. D. Friedman, J. Y. Lee, S. J. Kim, N. Kim, D. L. Dunner, and P. F. Renshaw, "Regional cerebral cortical thinning in biopolar disorder," *Bipolar Disorders*, vol. 8, pp. 65–74, 2006.

[6] M. Martinussen, B. Fischl, H. B. Larsson, J. Skranes, S. Kulseng, T. R. Vangberg, T. Vik, A. M. Brubakk, O. Haraldseth, and A. M. Dale, "Cerebral cortex thickness in 15-year-old adolescents with low birth weight measured by an automated MRI-based method," *Brain*, vol. 128, pp. 2588–2596, 2005.

[7] B. Hamann, "Curvature approximation for triangulated surfaces," in *Geometric Modelling in Computing Supplementum 8*, G. Farin, H. Hagen, and H. Noltemeier, Eds., pp. 139–153. Springer-Verlag, New York, 1993.

[8] E. W. Dijkstra, "A note on two problems in connection with graphs," *Numerische Mathematik*, vol. 1, pp. 269–271, 1959.

[9] J. A. McHugh, *Algorithmic Graph Theory*, Prentice Hall, New Jersey, 1990.

[10] M. Ono, S. Kubik, and A. Chad, *Atlas of the Cerebral Sulci*, G. Thieme Verlag, Stuttgart, 1990.

[11] P. Rogen and H. Bohr, "A new family of global protein shape descriptors," *Mathematical Biosciences*, vol. 182, pp. 167–181, 2003.

[12] F.B. Fuller, "The writhing number of a space curve," *Proceedings of the National Academy of Sciences of the United States of America*, vol. 68, no. 4, pp. 815–819, 1971.

[13] Y. Diao, C. Ernst, and J. V. Rensburg, "Thicknesses of knots," *Math. Proc. Camb. Phil. Soc.*, , no. 126, pp. 293–310, 1999.

[14] O. Gonzalez and J. H. Maddocks, "Global curvature, thickness, and the ideal shapes of knots," *Proc. Natl. Acad. Sci. (USA)*, , no. 96, pp. 4769–4773, 1999.

[15] C.-H. Lo and H.-S. Don, "Representation and recognition of 3D curves," in *Proceedings IEEE Computer Society Conference on Computer Vision and Pattern Recognition*. IEEE, 1989, pp. 523–528.

[16] J.-F. Mangin, F. Poupon, E. Duchesnay, D. Rivière, A. Cachia, D. L. Collinse, A.C. Evans, and J. Régis, "Brain morphometry using 3D moment invariants," *Medical Image Analysis*, vol. 8, pp. 187–196, 2004.

[17] G. J. McLachlan, *Discriminant Analysis and Statistical Pattern Recognition*, Wiley, New York, 1992.

[18] Richard O. Duda, David G. Stork, and Peter E. Hart, *Pattern Classification*, John Wiley, Inc., Indianapolis, IN, 1999.

[19] I. H. Witten and E. Frank, *Data Mining: Practical machine learning tools and techniques*, Morgan Kaufmann, San Francisco, 2nd edition, 2005.